

AD-A127219

AD

AD-E400 998

TECHNICAL REPORT ARLCD-TR-83015

THE BURNING BEHAVIOR OF TNT IN THE CLOSED BOMB

RODOLF W. VELICKY

MARCH 1983



US ARMY ARMAMENT RESEARCH AND DEVELOPMENT COMMAND
LARGE CALIBER
WEAPON SYSTEMS LABORATORY
DOVER, NEW JERSEY

APPROVED FOR PUBLIC RELEASE; DISTRIBUTION UNLIMITED.

FILE COPY

DTIC
ELECTE

APR 05 1983

Best Available Copy

The views, opinions, and/or findings contained in this report are those of the author(s) and should not be construed as an official Department of the Army position, policy, or decision, unless so designated by other documentation.

Destroy this report when no longer needed. Do not return to the originator.

UNCLASSIFIED

SECURITY CLASSIFICATION OF THIS PAGE (When Data Entered)

REPORT DOCUMENTATION PAGE		READ INSTRUCTIONS BEFORE COMPLETING FORM
1. REPORT NUMBER Technical Report ARLCD-TR-83015	2. GOVT ACCESSION NO. AD-A127 279	3. RECIPIENT'S CATALOG NUMBER
4. TITLE (and Subtitle) THE BURNING BEHAVIOR OF TNT IN THE CLOSED BOMB		5. TYPE OF REPORT & PERIOD COVERED
		6. PERFORMING ORG. REPORT NUMBER
7. AUTHOR(s) Rodolf W. Velicky		8. CONTRACT OR GRANT NUMBER(s)
9. PERFORMING ORGANIZATION NAME AND ADDRESS ARRADCOM, LCWSL Energetic Materials Div (DRDAR-LCE) Dover, NJ 07801		10. PROGRAM ELEMENT, PROJECT, TASK AREA & WORK UNIT NUMBERS 1L162603AH18
11. CONTROLLING OFFICE NAME AND ADDRESS ARRADCOM, TSD STINFO Div (DRDAR-TSS) Dover, NJ 07801		12. REPORT DATE March 1983
14. MONITORING AGENCY NAME & ADDRESS (if different from Controlling Office)		13. NUMBER OF PAGES 33
		15. SECURITY CLASS. (of this report) Unclassified
		15a. DECLASSIFICATION/DOWNGRADING SCHEDULE
16. DISTRIBUTION STATEMENT (of this Report) Approved for public release; distribution unlimited.		
17. DISTRIBUTION STATEMENT (of the abstract entered in Block 20, if different from Report)		
18. SUPPLEMENTARY NOTES		
19. KEY WORDS (Continue on reverse side if necessary and identify by block number) TNT Combustion Burning Deflagration Closed bomb		
20. ABSTRACT (Continue on reverse side if necessary and identify by block number) The work shows that the physical structure of TNT breaks up during burning. Combustion proceeds on fragments with a new surface to volume ratio. The size, shape, and number of fragments is determined by the crystal pattern permitted to develop by the casting procedure. The intrinsic burning rate of TNT is very slow in relation to the rate of structural dissociation. Wax, the desensitizing agent used with TNT in the mixture Comp B, does not interact with TNT to modify its burning behavior.		

DD FORM 1 JAN 73 1473

EDITION OF 1 NOV 65 IS OBSOLETE

UNCLASSIFIED

SECURITY CLASSIFICATION OF THIS PAGE (When Data Entered)

SECURITY CLASSIFICATION OF THIS PAGE(When Data Entered)

SECURITY CLASSIFICATION OF THIS PAGE(When Data Entered)

ACKNOWLEDGMENT

Sincere appreciation is expressed to Dr. D. Downs of the Applied Science Division for the generous cooperation which made the performance of this work possible. Special gratitude is extended to Mr. Peter Cagiano, also of the Applied Science Division, for the help and technical assistance that he provided.

Accession For	
NTIS GRA&I	<input checked="" type="checkbox"/>
DTIC TAB	<input type="checkbox"/>
Unannounced	<input type="checkbox"/>
Justification	
By	
Distribution/	
Availability Codes	
Dist	Avail and/or Special
A	



CONTENTS

	Page
Introduction	1
Experimental	1
Instrumentation	1
Procedure	2
Results and Discussion	2
Test for Surface Area Burning, Cast TNT	2
Test for Surface Area Burning, Pressed TNT	3
Crushed and Flake TNT Compared with the Solid Grain	3
TNT with 2.5 Percent Wax Additive Compared with Cast TNT	3
Test for Melting or Fragmentation of TNT	4
Effect of Crystal Structure on the Burning of Cast TNT	5
The Effect of Density on the Burning of Pressed TNT	5
Conclusions	5
Recommendations	6
References	7
Distribution List	23

TABLES

	Page
1 Surface burning test for cast TNT	9
2 Surface Burning Test for pressed TNT	10
3 Effect of an increased surface area to volume ratio, cast TNT	11
4 Test for interaction of wax with TNT	12
5 Test for deconsolidation of physical structure of cast TNT	13
6 Effect of crystal structure on burning of TNT	14
7 Effect of density on burning of pressed TNT	15

FIGURES

1 Cast TNT, test for surface burning	17
2 Pressed TNT, test for surface burning	17
3 Crushed, flake, and solid TNT	18
4 TNT, with and without wax	18
5 Restricted surface area cups	19
6 Fragmentation burning test	19
7 Crystal structure burning test	20
8 Density effect, pressed TNT	20
9 Density versus quickness correlation	21

INTRODUCTION

TNT burns in an anomalous manner. Contrary to the burning behavior of gun propellants, cast and pressed samples react at a rate that is essentially independent of the initial geometrical configuration, i.e., surface area to volume ratio. Since TNT is used in large caliber explosive filled projectiles, and is a major constituent of the explosive Comp B, it is important to understand its idiosyncracies in order to unravel the anomalous burning characteristics reported for it and for Comp B (ref 1).

This work identifies the major factors controlling TNT's burning mechanism and provides a foundation for subsequent evaluation of its role in the combustion process of Comp B. It is intended as a broad overview, with the conclusions providing guidelines for further study.

EXPERIMENTAL

Closed bomb data, in relation to gun propellant linear burning rate regression theory, provided the foundation for this work. The theory states that the burning rate is an intrinsic property of the composition. Utilizing suitable techniques, the burning rate equation can readily be calculated from closed bomb pressure versus time data. The method is routinely used to evaluate gun propellant formulations (ref 2).

If a sample burns only on its exterior surface after the entire surface area is simultaneously ignited, essentially the same constants are developed for the equation:

$$r = ap^n$$

for any known geometrical configuration. When the same constants are not developed, for samples with different surface area to volume ratios (S_o/V_o), it means that the samples are burning on a surface area that is different than that predicted by linear regression of the initial surface area. This can happen through the fragmentation of the physical structure, penetration of burning into a porous body, or distortion of the surface area by massive melting.

When experiments are designed with specific goals, insight into unusual burning behavior can be gained from analysis of the quickness curve (dp/dt vs pressure). These curves are particularly useful when used to compare the effect of controlled differences, i.e., surface area, density, crystal size composition, etc. Based on the design of the experiment, valid inferences on the cause and effect relationship can be made.

Instrumentation

Details of the method are described in reference 1. Briefly stated, a heavy-walled vessel was provided with a closure, insulated firing electrode, and an exhaust valve. The pressure-versus-time data of a burning sample was sensed

with a piezo pressure transducer, collected with a Nicolett Explorer III digital oscilloscope, and permanently stored on magnetic discs. The data was then easily retrieved and processed with a Hewlett-Packard HP-85 desk top computer for various listings and plots.

Procedure

Some results on cast and pressed TNT are reported in reference 1. These results and data on crushed TNT, flake TNT, and TNT cast with wax will be discussed in more detail. This group of experiments was performed in a 201 cm³ (12.27 in³) bomb on single grain cylindrical samples. Questions stimulated by these experiments were addressed by a second group of experiments in a 252 cm³ (15.38 in³) vessel on samples burned under partial confinement in steel cups.

Precise cylindrical geometries were machined for cast TNT, pressed TNT, and TNT with wax. They were machined to provide two significantly different surface area to volume ratios for each sample. They were 2.54 cm (1.000 in.) diameter cylinders. One was solid and the other, a single perforated grain, contained a 0.953 cm (3/8 in.) diameter hole in the center. The lengths were adjusted to provide a constant mass, and were approximately 5 cm (2 in.) long. Crushed and flake forms of TNT were also tested. Each test was provided with massive thermal ignition by 5 grams of class 7 black powder. This was done to insure simultaneous ignition of the entire surface area.

RESULTS AND DISCUSSION

Test for Surface Area Burning, Cast TNT

The purpose of this experiment was to determine whether or not cast TNT burns by regression that is normal to its exterior surface. If this occurred, the two different geometries, described in Experimental, would generate the same constants for the linear burning rate equation. The quickness curve (dp/dt vs pressure), which provided the foundation for the calculation, must vary with respect to the surface area as a function of the volume fraction burned in order for the calculations to apply. The quickness curves for each of the two geometries were identical (fig. 1) (table 1). The solid and 3/8 single perforated grains are represented, respectively, by dotted and solid lines.

A common burning rate equation could not be generated for the two geometries. This could only mean that the physical structure has changed and provided a new surface area that is not represented by the original geometry. This can only be explained by the creation of a new common surface area from the initial geometries. This can happen through the complete breakup of TNT's physical structure or through its deformation, as might occur through massive melting.

Test for Surface Area Burning, Pressed TNT

Essentially, the same conclusions were drawn for pressed TNT as were drawn for cast TNT. The quickness curves for pressed TNT also show that a surface area alteration had taken place which produces similar burning from the two different geometries (fig. 2) (table 2).

Even though the density of the pressed TNT (1.59 g/cm^3) was slightly higher than the cast TNT (1.56 g/cm^3), it should be noted that it burns at a considerably slower rate than the cast TNT. This is an important observation and will be addressed by later experiments.

Crushed and Flake TNT Compared with the Solid Grain

Equal masses of crushed and flake TNT were also burned. Material from the same TNT casting was physically crushed into an aggregate of fine powder and small chunks. The flake TNT was thin oblong material [approximately $0.953 \text{ cm} \times 0.079 \text{ cm}$ ($3/8 \text{ in.} \times 1/32 \text{ in.}$)] from which all the castings were made. Although their surface to volume ratios (S_o/V_o) were not determined. This ratio was two to three orders of magnitude greater than each machined grain. The ratio for the crushed form was estimated to be at least ten times greater than the flake form. Figure 3, table 3, compares the quickness of crushed and flake TNT with the cast solid cylindrical grain.

All things being equal (mass, composition, etc.), the quickness (dp/dt) is directly related to the surface area burning. This comparison shows that the crushed TNT, with a surface area on the order of a thousand times greater than its solid cylindrical form burns only 20% faster. This strongly reinforces the conclusion drawn earlier that TNT is changing its surface area through fracturing and/or melting its physical structure.

Based on the tests performed thus far and the S_o/V_o relationship of the crushed and flake forms, one would expect the flake TNT to burn equal to or slower than the crushed TNT. In spite of having a smaller initial surface area, the flake TNT, surprisingly, burned faster than its recast crushed version. This suggested that the burning characteristics of TNT had been changed by the melting and recasting process. This point will be addressed by later experiments.

TNT with 2.5% Wax Additive Compared with Cast TNT

The 1% wax additive in Comp B significantly effected its burning behavior (ref 1). In order to determine if this effect was due to an interaction of the wax with TNT, an attempt was made to mix an equivalent quantity (2.5%) directly into the TNT. This was very difficult. In the melt, the wax appeared to be unmixable with the TNT. However, the mixture was homogenized and quickly cooled to lock the wax within the TNT casting. The waxy feel of the machined casting and the change in physical appearance indicated that a significant quantity of wax was locked in the casting.

Figure 4 compares the solid cylinder geometry of cast TNT with the solid cylinder geometry of TNT with added wax. There was no significant difference in

the results. TNT burned essentially the same with or without wax. The question of the role of wax in the combustion of Comp B will be addressed in a future report.

In table 4, the two geometrical forms of TNT are compared. The same independence of geometry behavior, previously noted for cast and pressed TNT, is observed for TNT with wax.

Test for Melting or Fragmentation of TNT

The previous experiments show that the physical structure of TNT changes independently of the original configuration during burning. This experiment was designed to indicate whether this change is due to melting or fragmentation (breakup) of the physical structure. Equal masses of TNT were cast in open cylindrical steel cups that should permit burning on only one surface. The surface provided by one set of cups was 3.81 cm (1.5 in.) in diameter and the other was 1.91 cm (0.75 in.) in diameter (fig. 5). These samples were ignited with 3 grams of class 7 black powder within a "Parr" high pressure bomb.

If TNT melts during burning, it is assumed that it will remain in the cup and the burning will take place on the restricted surface area defined by the diameter of the cup. The rate of burning would be related to the ratios of the surface areas. The TNT in the large diameter cup would burn faster than that in the small diameter cup and it should be possible to calculate TNT's linear burning rate.

If TNT was burning through a fragmentation process, it was expected that the quickness curves would be, as previously observed, the same for the two geometries. The results are shown in figure 6 and table 5.

The reverse of what should happen for a melting mechanism occurred. The sample with the smaller surface area actually burned faster. These results eliminate the melting mechanism as a possible explanation for the observations. It is therefore inferred that TNT burns predominantly by the decomposition of its physical structure. Fragments are created at an extremely rapid rate in relation to the burning time of the fragments. This is indicated because the quickness curves for the two machined geometries (cast and pressed) are virtually identical. If the fragments were created at a rate that was within their total burning time, there would be a meaningful difference between the two curves.

The quickness curves for the TNT burned in the two cup sizes does not conform to that expected for the fragmentation mechanism. The two quickness curves were expected to be identical; instead, samples with the small surface area burned faster. Fortunately before the burning, it had been noticed that this casting, because of a slow rate of cooling, had permitted the growth of a long, needle-like, crystal pattern. The larger diameter casting had been fast-cooled. Its crystal pattern was not visually structured.

Effect of Crystal Structure On The Burning of Cast TNT

Through serendipity it was indicated that TNT's crystal formation procedure had a significant effect on its burning behavior. In order to test this observation castings were made in the large diameter cup. One group was permitted to cool rapidly, while the other was allowed to crystalize slowly over a period of several hours. The quickly cooled casting had again, a visually undefined crystal structure, whereas the slowly cooled sample had a radially oriented pattern of long thin crystals. The result of the burnings are shown in figure 7 and table 6. The TNT with the long, thin, needle-like, crystal structure burned much faster than its unstructured counterpart.

The Effect of Density on the Burning of Pressed TNT

Although the densities were not comparable, it has been observed in a previous experiment that pressed TNT burned significantly slower than cast TNT. In order to clarify the meaning of this observation, a spectrum of densities were pressed into the larger diameter metal cups. The quickness of these samples is related to the density (fig. 8), (table 7). It is ranked in inverse order of the pressed density; it increased as density decreased. A good correlation is shown between the maximum dp/dt and the density (fig. 9).

That density can increase with loading pressure, means that there are voids (porosity) in the material that became smaller with respect to the applied load. The fact that TNT could be pressed to higher densities, than usually occur in good castings, indicates that collapsible fissures are present in TNT castings. It is quite possible that as the density of TNT approaches its maximum theoretical density (TMD), the intrinsic burning rate of the composition would become measurable. This would be an interesting area for future study.

CONCLUSIONS

1. The physical structure of TNT breaks up during the burning process. Fragments are rapidly created with a new, unknown, surface-to-volume ratio. The rate at which the structure dissociates is much faster than the intrinsic burning rate of the released fragment. The reactions combine the rate at which the physical structure dissociated, the surface-to-volume ratio of newly created fragment and the intrinsic burning rate of the composition.

2. The size, shape, and number of fragments is determined by the crystal pattern permitted to develop by the casting procedure.

3. Porosity was the major factor controlling the burning process in pressed TNT. Collapsible fissures (voids) that occurred naturally could exist in cast TNT. This was indicated by the fact that TNT could be easily pressed to higher densities than normally obtained in casting.

4. Porosity alone did not appear to provide a sufficient reason for the dissociation of the physical structure of TNT at the observed rapid rate. However, the existence of crystal patterns implies that there are boundary layers between neighboring crystals. These are areas of weakness, which could provide cleavage paths for dissociation of the structure. The inferred, built-in porosity might be associated with this boundary layer.

5. Wax did not interact with TNT to modify its burning characteristics.

RECOMMENDATIONS

There are several parameters associated with the deconsolidating burning mechanism that are combined in the quickness measurement. They are the rate of structure dissociation, the average surface area of the dissociating fragment, and the intrinsic burning rate of the composition. Separated and measured, this data would provide a basis for understanding the deflagration side of the deflagration to detonation (DDT) mechanism.

Well-designed experiments utilizing the closed bomb could help separate these unknowns. Researchers should be encouraged and supported to use the close bomb in the investigation of explosive burning. It is an extremely versatile tool that is not used in proportion to its value.

REFERENCES

1. R.W. Velicky and J. Herchkowitz, "Anomalous Burning Rate Characteristics of Composition B and TNT", Seventh Symposium (International) on Detonation, 1981.
2. A. Pallington and M. Weinstein, "Method of Calculation of Interior Ballistic Properties of Propellants from Closed Bomb Data", Picatinny Arsenal Technical Report 2005, Picatinny Arsenal, Dover, NJ, June 1954.

Table 1. Surface burning test for cast TNT

Pressure (MPa)	Quickness (MPa/ms)		
	#1	#2	#3
<u>Solid Cylinder</u>			
30	5.57	5.59	5.56
40	7.80	7.83	9.31
50	10.82	10.05	10.51
60	14.64	13.14	14.31
70	17.32	16.65	17.07
80	19.36	17.82	18.51
90	20.63	19.59	20.49
100	22.99	21.99	22.69
110	24.32	23.25	24.32
120	26.14	25.39	26.53

<u>3/8 ID Single Perforated</u>			
30	5.14	4.95	4.4
40	6.03	6.51	5.36
50	9.34	8.35	8.76
60	12.07	11.73	11.72
70	15.16	15.19	14.99
80	17.78	16.90	18.02
90	19.71	19.07	19.11
100	21.49	21.33	21.49
110	22.47	23.30	23.24
120	24.47	24.89	24.67

Table 2. Surface burning test for pressed TNT

Pressure (MPa)	Quickness (MPa/ms)		
	#1	#2	#3
<u>Solid Cylinder Geometry</u>			
(Density = 1.59 g/cc)			
30	1.56	1.43	2.30
40	3.65	4.09	3.21
50	5.06	5.66	5.76
60	6.94	7.53	6.93
70	7.82	8.23	7.59
80	9.53	10.42	10.11
90	11.62	11.90	11.22
100	12.95	14.44	13.78
110	14.76	17.43	15.78
120	16.70	19.75	17.51
<u>3/8 ID Single Perforation Geometry</u>			
(Density = 1.59 g/cc)			
30	1.37	2.26	2.49
40	2.70	2.61	2.92
50	4.49	4.62	5.21
60	6.53	6.41	6.57
70	7.55	7.33	8.17
80	10.20	8.81	10.29
90	11.91	10.65	12.39
100	14.05	12.93	14.57
110	16.63	15.34	17.29
120	18.63	17.12	19.35

Table 3. Effect of an increased surface area to volume ratio, cast TNT

<u>Pressure</u> (MPa)	<u>Quickness</u> (MPa/ms)	
	<u>#1</u>	<u>#2</u>
	<u>Crushed TNT</u>	
30	9.96	10.69
40	12.09	13.16
50	13.99	15.96
60	16.81	19.21
70	19.89	22.42
80	22.77	24.99
90	25.30	27.11
100	27.52	28.89
110	29.35	30.18
120	30.62	31.05
	<u>Flake TNT</u>	
30	13.33	14.97
40	16.70	17.12
50	20.61	19.72
60	24.30	22.57
70	27.25	25.39
80	29.78	28.06
90	31.79	30.57
100	33.68	32.91
110	35.28	34.95
120	36.63	36.68

Table 4. Test for interaction of wax with TNT

Pressure (MPa)	Quickness (MPa/ms)		
	#1	#2	#3
<u>Solid Cylinder Geometry</u>			
(Cast with 2.5% wax)			
30	4.28	4.87	4.80
40	6.53	8.02	8.24
50	9.36	11.54	11.49
60	11.34	13.07	14.34
70	15.41	14.20	15.27
80	19.19	17.24	17.38
90	21.71	20.59	20.46
100	23.53	23.30	23.43
110	25.05	25.42	25.63
120	26.29	26.86	26.90

3/8 ID Single Perforation Geometry

(Cast with 2.5% wax)

30	2.73	2.41	1.74
40	7.75	5.98	4.12
50	12.17	9.42	8.24
60	15.57	12.16	13.26
70	17.21	13.74	16.22
80	17.84	15.86	18.59
90	19.66	19.44	20.76
100	22.16	33.01	22.82
110	24.33	35.10	24.65
120	25.61	25.88	26.08

Table 5. Test for the deconsolidation of the physical structure of cast TNT

Pressure (MPa)	Quickness (MPa/ms)	
	#1	#2
<u>Diameter Cup, 1.500 inch</u>		
10.0	35.5	37.6
12.5	61.9	66.5
15.0	109.3	107.3
7.5	176.7	159.0
20.0	231.9	211.5
22.5	274.4	260.2
25.0	316.8	311.1
27.5	353.8	354.9
30.0	381.6	392.4
32.5	405.4	418.0
35.0	408.9	426.0
37.5	382.2	419.2
40.0	335.9	388.6

Diameter Cup, 0.750 inch

10.0	103.6	104.5
12.5	162.0	243.6
15.0	210.0	283.6
17.5	276.1	320.3
20.0	423.0	348.3
22.5	443.5	397.8
25.0	477.4	448.8
27.5	529.3	390.6
30.0	598.3	530.9
32.5	629.1	556.2
35.0	611.5	558.6
37.5	556.8	516.1
40.0	444.2	414.0

Table 6. Effect of crystal structure on burning of TNT

Pressure (MPa)	Quickness (MPa/ms)	
	#1	#2
<u>Short Crystal Structure</u>		
10.0	29.5	26.2
12.5	45.9	34.2
15.0	79.2	54.2
17.5	113.0	84.1
20.0	159.5	113.7
22.5	198.8	148.7
25.0	246.3	178.9
27.5	291.8	205.6
30.0	324.9	236.5
32.5	349.9	261.5
35.0	369.3	281.4
37.5	359.9	290.4
40.0	344.1	277.7
<u>Long Crystal Structure</u>		
10.0	123.1	67.7
12.5	220.5	138.5
15.0	292.6	241.2
17.5	385.0	327.8
20.0	432.8	394.0
22.5	506.8	471.6
25.0	574.8	553.7
27.5	637.8	645.7
30.0	684.9	714.1
32.5	740.7	769.0
35.0	745.0	825.3
37.5	732.5	849.5
40.0	662.6	839.0

Table 7. Effect of density on burning of pressed TNT

Pressure MPa	Quickness MPa/s				
	<u>1.510</u> <u>(g/cc)</u>	<u>1.525</u> <u>(g/cc)</u>	<u>1.559</u> <u>(g/cc)</u>	<u>1.604</u> <u>(g/cc)</u>	<u>1.664</u> <u>(g/cc)</u>
10.0	204.4	95.1	18.7	32.5	25.7
12.5	391.5	196.7	52.5	55.0	32.6
15.0	542.5	327.6	84.6	103.8	38.8
17.5	546.3	461.3	163.9	152.7	51.2
20.0	772.4	520.6	265.9	197.9	62.3
22.5	863.7	571.1	349.2	244.2	76.3
25.0	960.6	641.5	420.2	309.6	91.4
27.5	1041.1	712.8	495.8	360.7	104.2
30.0	1113.7	781.0	571.3	400.3	120.3
32.5	1157.1	828.5	645.3	426.6	132.8
35.0	1177.7	860.8	688.4	446.6	136.8

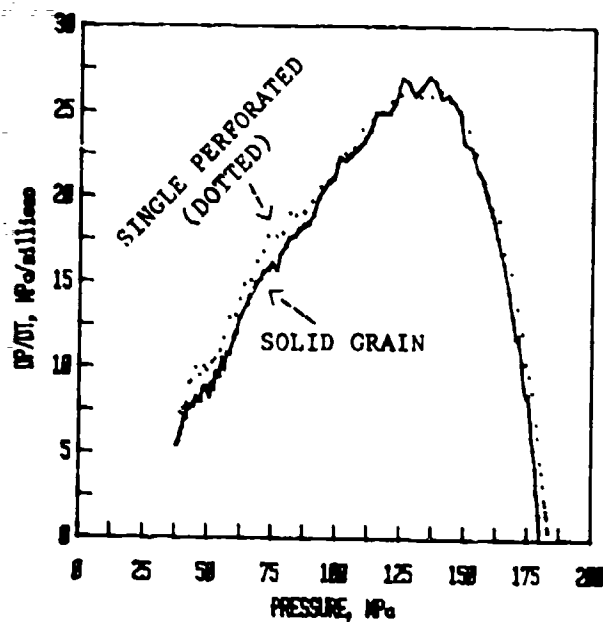


Figure 1. Cast TNT, test for surface burning (1.56 g/cm^3)

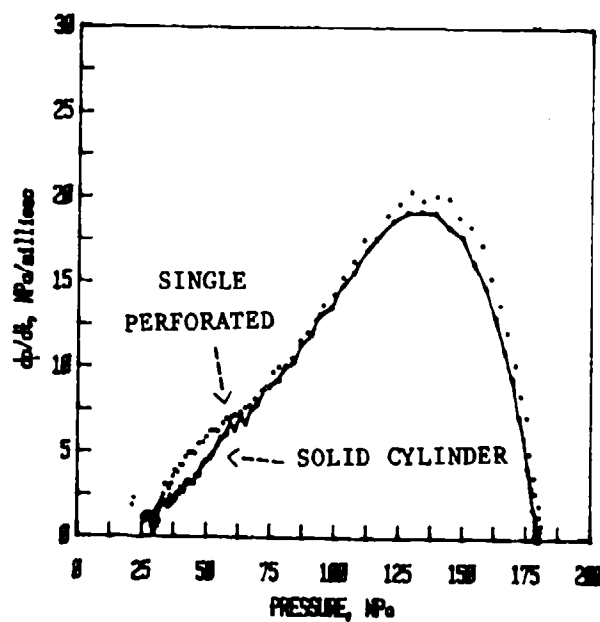


Figure 2. Pressed TNT, test for surface burning (1.59 g/cm^3)

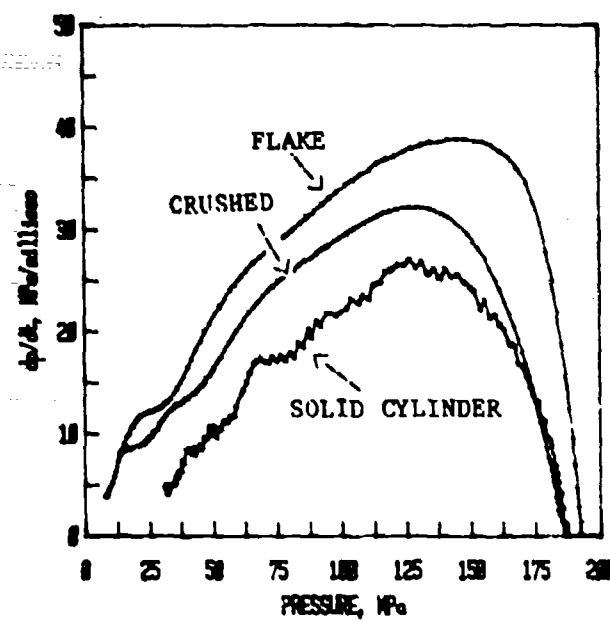


Figure 3. Crushed, flake, and solid TNT

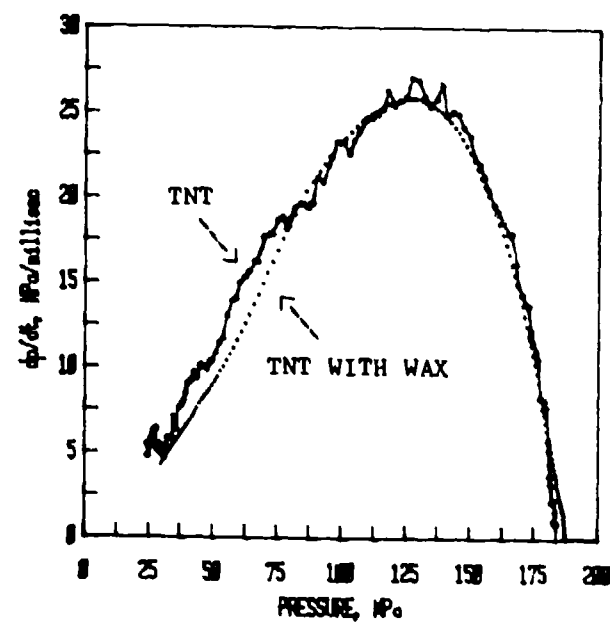


Figure 4. TNT, with and without wax

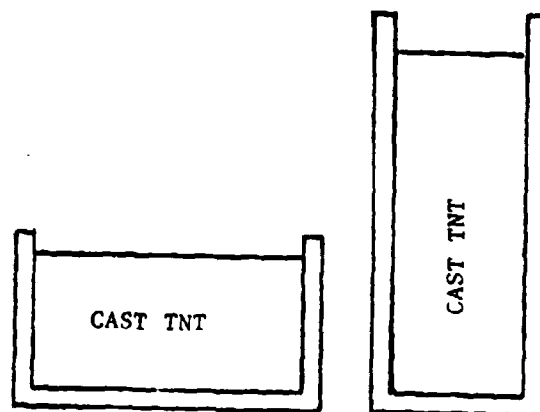


Figure 5. Restricted surface area cups

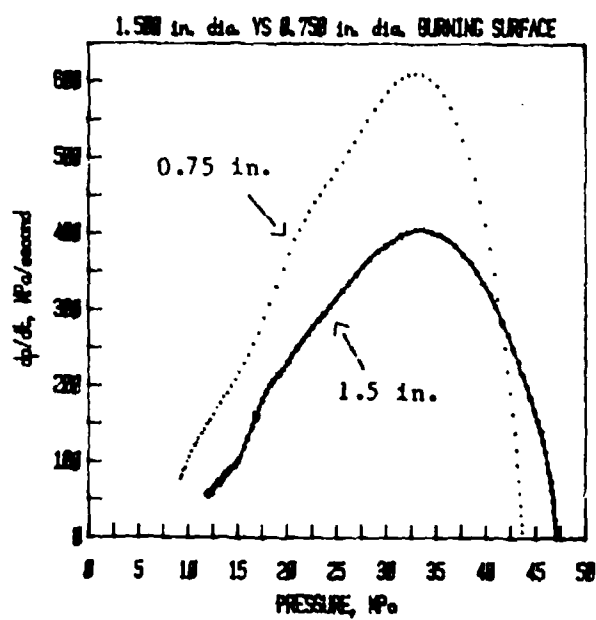


Figure 6. Fragmentation burning test

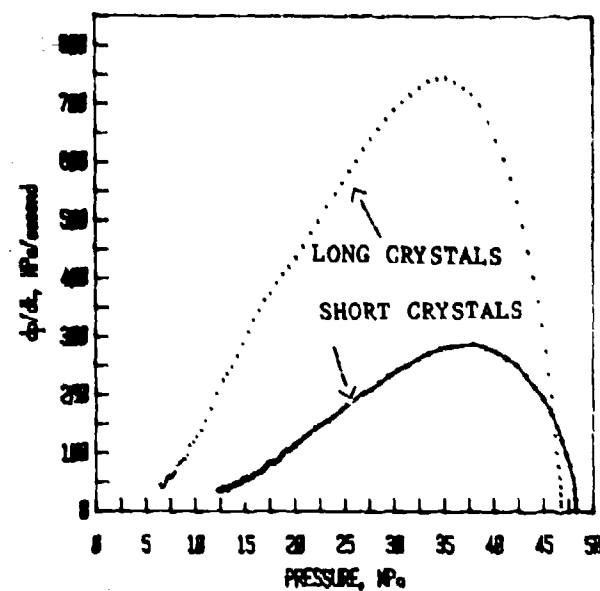


Figure 7. Crystal structure burning test

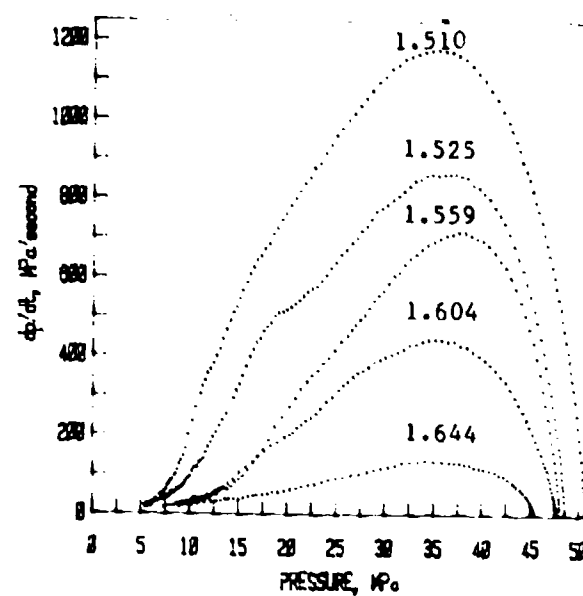
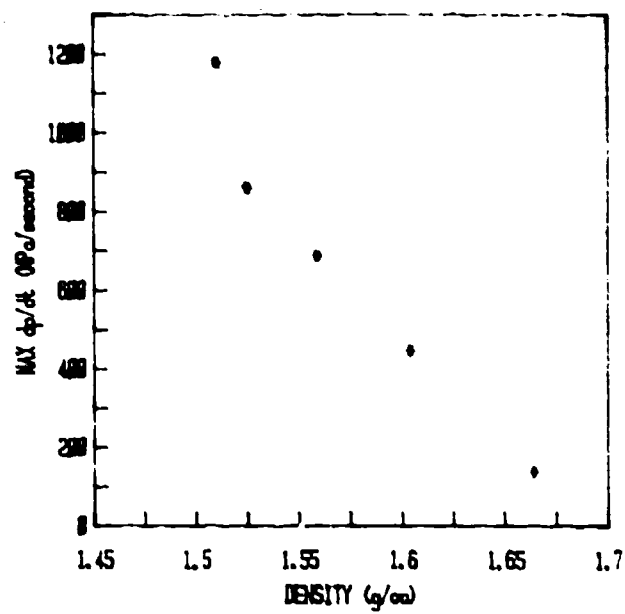


Figure 8. Density effect, pressed TNT



CORRELATION OF QUICKNESS WITH PRESSED DENSITY

Figure 9. Density versus quickness correlation

DISTRIBUTION LIST

Commander

U.S. Army Armament Research and
Development Command

ATTN: DRDAR-CG

DRDAR-GCL

DRDAR-LC

DRDAR-LCA, Dr. J. Lannon

Dr. D.S. Downs

Dr. A. Beardell

Dr. T. Vladimiroff

Mr. A. Grabowski

DRDAR-LCE, Dr. R.F. Walker (3)

DRDAR-LCE-D, Mr. R. Velicky (20)

DRDAR-LCM, Mr. L. Saffian

DRDAR-LCU, Mr. A. Moss

Mr. E.J. Zimpo

DRDAR-TDS, Mr. V. Lindner

DRDAR-TDC, Dr. D. Gyrog

WDAP-TSS (5)

J 07801

Administrator

Defense Technical Information Center

ATTN: Accessions Division (12)

Cameron Station

Alexandria, VA 22314

Director

U.S. Army Materiel Systems Analysis Activity

ATTN: DRXSY-MP

Aberdeen Proving Ground, MD 21005

Commander/Director

Chemical Systems Laboratory

U.S. Army Armament Research and
Development Command

ATTN: DRDAR-CLJ-L

DRDAR-CLB-PA

APG, Edgewood Area, MD 21010

Chief

Benet Weapons Laboratory, LCWSL

U.S. Army Armament Research and
Development Command

ATTN: DRDAR-LCB-TL

Watervliet, NY 12189

Director
Ballistics Research Laboratory
U.S. Army Armament Research and
Development Command

ATTN: DRDAR-BL, Dr. R.J. Eichelberger
DRDAR-IB, Dr. E. Freedman
Mr. N. Gerri
H. Reeves
A. Juhasz
DRDAR-TB, R. Vitali
P. Howe
R. Frey
I. May

DRDAR-TSB-S
Aberdeen Proving Ground, MD 21005

Commander
U.S. Army Armament Materiel
Readiness Command
ATTN: DRSAR-LEP-LM, R. Freeman
DRSAR-LEP-L
Rock Island, IL 61299

Director
U.S. Army TRADOC Systems
Analysis Activity
ATTN: ATAA-SL
White Sands Missile Range, NM 88002

Director
Industrial Base Engineering Activity
ATTN: DRXIB-MT
Rock Island, IL 61299

Office of Director of Defense
Research and Engineering
ATTN: R. Thorkildsen
Washington, DC 20301

Department of Defense
Explosives Safety Board
ATTN: R.A. Scott, Jr.
Washington, DC 20314

Director
Advanced Research Projects Agency
Department of Defense
Washington, DC 20301

Headquarters
Department of the Army
Office of Deputy Chief of Staff for
Research Development & Acquisition
Munitions Division
ATTN: DAM-CSM-CA
Washington, DC 20310

Commander
U.S. Army Materiel Development and
Readiness Command
ATTN: DRCDMD-ST (2)
DRCSF-E, Mr. McCorkle (2)
5001 Eisenhower Avenue
Alexandria, VA 22333

Director
U.S. Army Systems Analysis Agency
ATTN: J. McCarthy
Aberdeen Proving Ground, MD 21005

Director
DARCOM Field Safety Activity
ATTN: DRXOS-ES
Charlestown, IN 47111

Commander
Harry Diamond Laboratories
ATTN: Technical Library
Branch 420, R.K. Warner
2800 Powder Mill Road
Adelphi, MD 20783

Commander
U.S. Army Research Office
ATTN: H. Robl
Box CM, Duke Station
Durham, NC 27706

Commander
Naval Ordnance Station
ATTN: W. Vreatt
Safety Department
M.C. Hudson
Code 5251B, S. Mitchell
Technology Ctr, Code 5037,
P. Fields
Technical Library
Indian Head, MD 20640

Commander
U.S. Naval Sea Systems Command
ATTN: E.A. Daugherty
SEA-064E, Mr. R.L. Beauregard
SEA-62YC (2)
SEA-62Y13C
Washington, DC 20362

Commander
Naval Weapons Support Center
ATTN: Code 3031, Mr. D. Ellison
Crane, IN 47522

Commander
U.S. Naval Weapons Center
ATTN: A. Amster
T.B. Joyner
Code 45, C.D. Lind
Technical Library
Code 3273 (Weathersby)
China Lake, CA 93555

Commander
Naval Air Systems Command
ATTN: AIR-310C, H. Rosenwasser
AIR-52321A, W. Zuke
Washington, DC 20361

Commander
Naval Weapons Station
ATTN: W. McBride
L.R. Rothstein
Yorktown, VA 23491

Commander
Naval Coastal Systems Laboratory
J. Hammond, Code 722, Bldg 11C
J. Kirkland
E. Richards, Code 721
D.W. Shepherd, Code 741
Panama City, FL 32401

Commander
Naval Surface Weapons Center
ATTN: S. Nesbitt, R12
G. Laib, R12
Technical Library
Silver Spring, MD 20910

Assistant General Manager for
Military Applications
U.S. Atomic Energy Commission
Washington, DC 20543

Commander
Air Force Armament Development and Test Center
ATTN: AFB Technical Library
ADTC/DLIW, Dr. L. Elkins
DLDE, Mr. T.G. Floyd
Mr. G. Moy
Eglin Air Force Base, FL 32542

Director
U.S. Army Aeronautical Laboratory
Moffett Field, CA 94035
Bureau of Mines
ATTN: Mr. R.W. Watson
4800 Forbes Avenue
Pittsburgh, PA 15213

Director
NASA Ames Research Center
ATTN: Technical Library
Moffett Field, CA 94035

Director
Sandia Laboratories
ATTN: Dr. D. Anderson
Technical Library
Albuquerque, NM 87115

Lawrence Livermore Laboratory
ATTN: Technical Library
L402, Dr. R. McGuire
Dr. J.W. Kury
Dr. H.E. Rizzo
Dr. M. Finger
Dr. D. Orrnellas
P.O. Box 808
Livermore, CA 94550

Los Alamos Scientific Laboratory
ATTN: Technical Library
Dr. R.N. Rogers, WX-2
Dr. G. Seay, WX-7
Los Alamos, NM 87544

McDonnell Aircraft Company
Department 353, Bldg. 33
ATTN: Mr. M.L. Schimmel
St. Louis, MO 63166

Mr. Joseph Hershkowitz
305 Passaic Avenue
West Caldwell, NJ 07006

Bureau of Explosives
Association of American Railroads
ATTN: Dr. W.S. Chang
Raritan Center, Bldg. 812
Edison, NJ 08817

Princeton Combustion Research
Laboratories, Inc.
ATTN: Dr. M. Summerfield
1041 U.S. Highway One
Princeton, NJ 08540

Defense Logistics Studies
Information Exchange (2)
U.S. Army Logistics Management Center
Ft. Lee, VA 23801

Commander
Naval Surface Weapons Center
ATTN: G
G20
G23 (15)
G30
G33 (2)
G60
F56 (Gray)
N40
N41 (Hammer)
R11 (Mueller)
R12 (Mont)
R13
Dahlgren, VA 22448